Iraqi Journal of Science, 2025, Vol. 66, No. 9, pp: 3981-4000
DOI: 10.24996/ijs.2025.66.9.36

ISSN: 0067-2904

Assessing Landslide Susceptibility Using Analytical Hierarchy Process (AHP) and Frequency Ratio (FR) in the Oued Lebene Watershed, North Morocco

Fahed El Amarty[1]*, Afaf Chakir [2], Lahcen Benaabidate[1], Abderrahim Lahrach[1]
[1] *Functional Ecology and Environmental Engineering Laboratory (LEFGE), FST-Fes, Sidi Mohammed Ben Abdellah University, Immouzer Road, BP: 2202, Fez 30000, Morocco*
[2]*Innovative Materials and Mechanical Manufacturing Processes Laboratory (IMMM), ENSAM-Meknes, Moulay Ismail University, Marjane 2, BP: 15290 Meknes 50500, Morocco.*

Received: 31/5/2024 Accepted: 14/8/2024 Published: 30/9/2025

Abstract

Assessing landslide susceptibility is paramount in planning, implementing management plans, and mitigating risks in areas vulnerable to this hazard. The present study, based on the Analytical Hierarchy Process (AHP) and Frequency Ratio (FR) in conjunction with Geographic Information Systems (GIS), aims to evaluate landslide susceptibility in the Oued Lebene watershed. Eleven causal factors determining landslides were considered, including elevation, slope, aspect, curvature, relative relief, lithology, precipitation, distance to drainage, distance to road, NDVI, land use, and vegetation cover. Using both AHP and FR methods, a correlation between previous landslides and triggering factors was established to assess their influence on landslide susceptibility. Maps depicting sensitivity were produced using each method, categorized into four groups, and subsequently validated using the area under the curve (AUC). The AHP approach unveiled that regions characterized by high, moderate, and low susceptibility correspondingly constitute 21.24%, 70.57%, and 7.84% of the total area. Likewise, the FR technique suggests that regions with high, moderate, and low susceptibility comprise 2.50%, 39.39%, and 58.03% of the study area, respectively. The findings indicate that FR, with an AUC of 0.722, outperformed AHP, which achieved an AUC of 0.711, in delineating the study areas concerning historical landslides. These maps will be of valuable utility for planners and decision-makers for meticulous planning and risk mitigation purposes.

Keywords: Analytical Hierarchy Process, Frequency Ratio, landslide susceptibility, Northern Morocco, Oued Lebene watershed.

تقدير عرضة الانهيارات الأرضية باستخدام عملية التسلسل الهرمي التحليلي (AHP) ومعدل التكرار (FR) في الريف الوسطى (شمال المغرب): دراسة حالة حوض وادي لبن

فاهد العمارتي[1]*، عفاف شاكر[2]، لحسن بنعبيدات[1]، عبد الرحيم لحرش[1]

* Email : fahed.elamarty@usmba.ac.ma

[1]مختبر لعلم البيئة الوظيفي والهندسة البيئية
كلية العلوم والتقنيات – فاس، جامعة سيدي محمد بن عبد الله، طريق إيموزر، صندوق بريدي 2202، فاس 30000، المغرب
[2]مختبر للمواد المبتكرة وعمليات التصنيع الميكانيكي
المدرسة الوطنية العليا للفنون والمهن –مكناس، جامعة مولاي إسماعيل، مرجان 2، صندوق بريدي 15290، مكناس 50500، المغرب

الخلاصة

التنبؤ بالانهيارات الأرضية ضروري في التخطيط والحد من المخاطر في المناطق المعرضة لهذا الخطر. الدراسة الحالية، التي تعتمد على عملية التسلسل الهرمي التحليلي (AHP) ومعدل التكرار (FR) باستعمال نظم المعلومات الجغرافية (GIS)، تهدف إلى تقييم عُرضة الانهيارات الأرضية في حوض وادي لبن. حيث تم اعتبار أحد عشر عاملاً سببياً يحدد الانهيارات الأرضية، بما في ذلك الارتفاع، المنحدر، الجانب، الانحناء، الارتفاع النسبي، التركيبة الجيولوجية، كمية الأمطار، المسافة إلى الوديان، المسافة إلى الطريق، مؤشر النبات الطبيعي، استخدام الأراضي وتغطية النبات. من خلال تطبيق طرق AHP وFR، تم إنشاء تطابق بين الانهيارات الأرضية السابقة والعوامل المحفزة لتقييم تأثيرها على عُرضة الانهيارات الأرضية. تم إنتاج خرائط تصويرية توضح الحساسية باستخدام كل طريقة، مصنفة إلى أربع مجموعات، وتم التحقق منها بشكل لاحق باستخدام مساحة تحت المنحنى (AUC). كشفت عملية التسلسل الهرمي التحليلي AHP أن المناطق المميزة بالعُرضة العالية جداً، العالية، المعتدلة، والمنخفضة تشكل على التوالي 0.36%، 21.24%، 70.57%، و7.84% من المساحة الكلية. وبالمثل، يشير تقنية FR إلى أن المناطق ذات العُرضة العالية جداً، العالية، المعتدلة، والمنخفضة تمثل 0.08%، 2.50%، 39.39%، و58.03% من مساحة الدراسة على التوالي. تشير النتائج إلى أن تقنية FR، بمساحة تحت المنحنى (AUC) قدرها 0.722، قد تفوقت على تقنية AHP، التي حققت AUC قدرها 0.711، في تحديد المناطق المدروسة فيما يتعلق بالانهيارات الأرضية التاريخية. ستكون هذه الخرائط ذات فائدة قيمة للمخططين وصناع القرار للتخطيط الدقيق والحد من المخاطر.

الكلمات الرئيسية: عرضة الانهيارات الأرضية، عملية التسلسل الهرمي التحليلي، معدل التكرار، حوض وادي لبن، شمال المغرب.

1. Introduction

Landslides are defined as the movement of soil or rock masses downslope, resulting from interaction with gravitational force [1], [2]. This phenomenon is primarily caused by the interaction of factors such as intense soil weathering and significant precipitation, exacerbated by human intervention in the form of rapid urbanization and infrastructure development [3], [4], [5], [6]. On the other hand, the triggering of landslides in mountainous areas is determined by orographic parameters, including slope, aspect, curvature, relief magnitude, hydrology encompassing flow density, groundwater circulation, and distance to watercourses, geomorphology, land use, as well as seismicity considering earthquakes and volcanism [7], [8], [9], [10].

Landslides, recognized as natural disasters, inflict more significant damage than earthquakes and floods in certain regions [11]. Cause approximately 1,000 fatalities worldwide annually [12], [13], and result in material losses amounting to around 4 billion dollars due to slope failures [14]. Landslides account for 9% of all natural hazards [15]; they induce morphological alterations in the landscape while causing damage to natural and artificial soil structures [16].

Compared to Western countries, efforts to prevent risks and landslides in Morocco are less addressed [17]. The most notable work in this area was carried out during the implementation of the D.E.R.R.O project, where the agricultural administration became aware of the damages

caused to agricultural lands, silted dams due to significant alluvial loads originating from upstream Bad Lands, and the undermining of riverbanks, as well as damages affecting road infrastructure.

However, landslide risk mapping in Morocco only began in the early sixties after the establishment of geotechnical maps of some cities (Tangier, Fez, Rabat...) by researchers Humbert and Jeanette in 1962. Indeed, the first landslide hazard maps were established by Millies-Lacroix in 1968 for the Rif region, known for its exposure to this hazard, followed by the pre-Rif area as part of the development of the Sebou watershed (Avenard, 1969). Although these innovative documents are available, Moroccan engineers and researchers have shown limited interest in systematic studies, preferring to focus mainly on the punctual consolidation of road network slopes. One notable exception lies in the maps developed as part of doctoral theses, specifically for the regions of El Hoceima, Taounate, Tetouan, and the Tangier Peninsula.

Identifying areas with potential risk is crucial to mitigate the damages caused by landslides, whether of natural or anthropogenic origin, which have harmful consequences for human life, the natural environment, and the economy [14], [18]. The inaccessibility of locations and the unavailability of data make it challenging to assess high-potential landslide areas. However, currently, the application of GIS and the analysis of satellite images and Google Earth have enabled the identification and evaluation of potential landslide locations on steep and inaccessible slopes [19], [20], [21].

Given the destructive nature of landslides, numerous researchers have developed techniques to assess areas' susceptibility to landslides. These techniques are classified according to statistical [22], [23], probabilistic [24], [25], deterministic [26], and expertise-based approaches [27], [28], [29]

Although various approaches to assessing landslide susceptibility exist, a conclusive determination of the best method to adopt in different regions remains elusive. Within the realm of qualitative approaches, the Analytic Hierarchy Process (AHP) is generally acknowledged as the preferred approach for analyzing landslide susceptibility, relying on the knowledge and expertise of experts. The integration of the AHP has undergone significant transformation since its introduction by Saaty (1977) as a new methodology for mapping landslide susceptibility zones. Many applications of this method have been reported in various regions worldwide [30], [31], [32]. Some studies have also conducted comparisons between the Factor Rating (FR) and (AHP) methods for assessing landslide susceptibility [27], [33], [34], [35]. However, no studies have been reported concerning this specific facet in watersheds.

Landslide susceptibility map models were developed to address this gap by combining the AHP and Factor Rating (FR) approaches. This fusion allowed for the weighting of all causal factors by class. Afterward, the precision and dependability of these models were evaluated by employing the area under the curve and juxtaposed the outcomes of AHP and FR regarding their efficacy in assessing landslide susceptibility in Oued Lebene.

2. Methods and Materials

2.1 The Study Area

The Oued Leben watershed, situated within the larger Sebou River basin in Morocco, covers a total area of 1386 km² and is located on the southern slope of the pre-Rif region (Fig.1). It is elongated in shape and oriented NNE-SSW, stretching over several tens of

kilometers, with variations in elevation over short distances [36]. Primarily drained by the Oued Leben River, which extends for 67.39 km, it lies within the transitional Rif's geological zone between the high mountains of the southern Rif, reaching a maximum altitude of 1700 m, and the low hills of the eastern and central pre-Rif region, with a minimum altitude of 300 m.

From a geological perspective, the watershed is characterized by various formations, including sedimentary sequences and rock outcrops. The lithology upstream of the watershed reveals the presence of various layers, including black pelites with rare small sandstone beds and intercalations of clayey limestone from the Cretaceous period, and black flysch with a pelitic dominance and rare limestone beds from the Upper Jurassic. Downstream, the study area is dominated by formations consisting of marls, marly limestones, intraformational conglomerates, and oolitic limestone with flint from the Lias period. Additionally, conglomerates and detrital limestones from the Middle Miocene are present [37].

Precipitation in the region is closely associated with the Mediterranean climate, characterized by distinct seasons of cold winters and dry summers. The wet season typically lasts from November to May. Annual rainfall ranges between 600-1013 mm/year, exhibiting significant variability, which results in seasonal fluctuations in the flow of the Oued Lebene watershed.

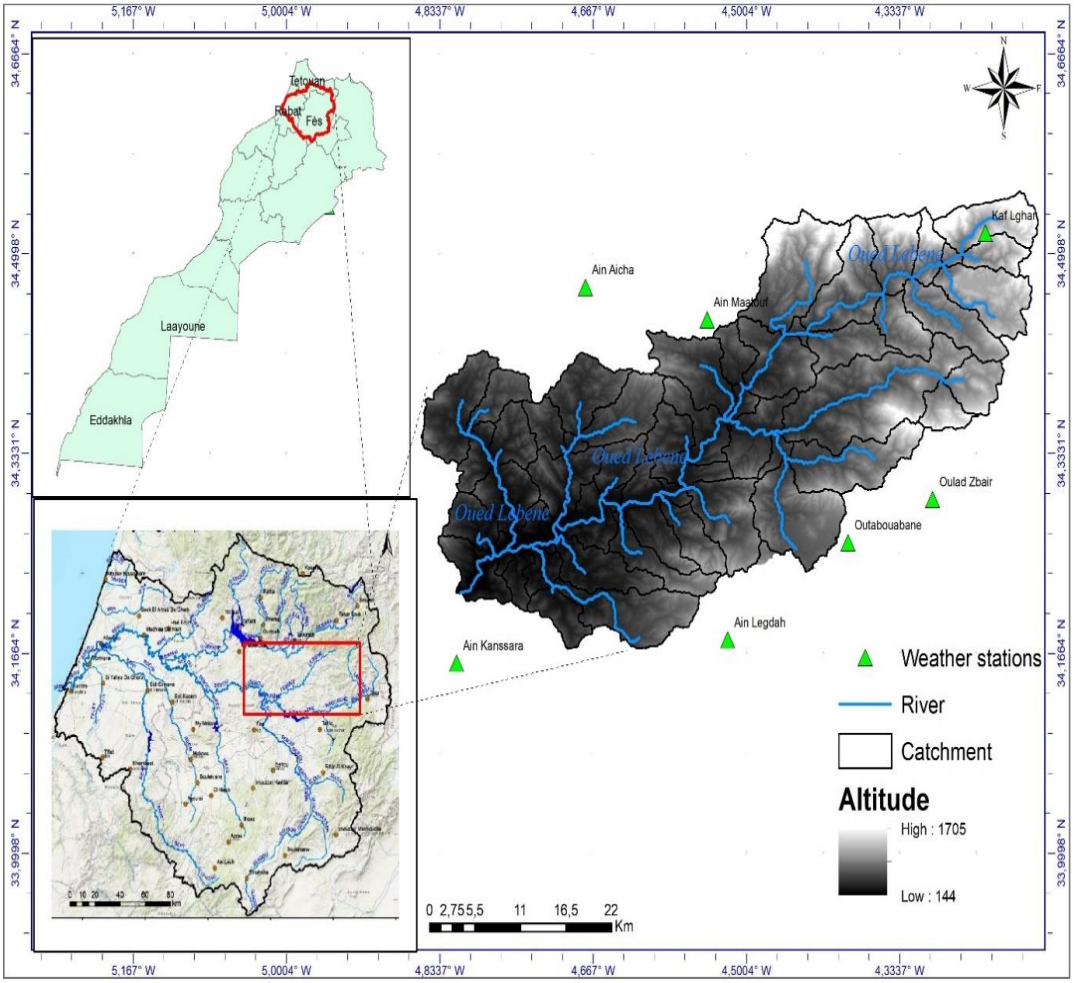

Figure 1: Location map of the Oued Lebene watershed

2.2 Methodologies and data sets

The data required for this study were collected from various sources. A geological map of the Rif (1/500,000 scale), meteorological data, an ASTER Digital Elevation Model (DEM), and a Landsat-8 image dated 03/05/2023 were utilized. Climatic data covering 30 years of the regional directorate of agriculture and the water and forestry services of the Fes-Meknes region provided (1992-2022). Additionally, a Landsat-8 image with a resolution of 30 m was obtained from the United States Geological Survey (USGS) website, and an ASTER DEM with a resolution of 30 m was retrieved from the NASA Earth Explorer website (Table 1).

Table 1: Data Sources

Data	Resolution / Scale	Source
DEM	30 * 30	https://earthexplorer.usgs.gov
Landsat 8	30 * 30	https://earthexplorer.usgs.gov
Elevation	30 * 30	Derived from the DEM
Slope	30 * 30	Derived from the DEM
Aspect	30 * 30	Derived from the DEM
Curvature	30 * 30	Derived from the DEM
Relative Relief	30 * 30	Derived from the DEM
Stream Map	30 * 30	Derived from the DEM
LULC	30 * 30	Derived from the Landsat 8
NDVI	30 * 30	Derived from the Landsat 8
Lithology	1/500000,Rasterization 30 * 30	digitization of the geological map of Rif
Rainfall	Interpolation with 30 * 30	The regional agriculture department (DRA) and the water and forestry services (ANEF) of the Fes-Meknes region
Roads Map	1/50000,Rasterization 30 * 30	digitization of Dhar Souk, Taineste, Kalaa des Sles, Tissa, Beni Frassen et Bab Lmrouj topographic maps 1/50000

This study was initiated by designing a detailed inventory map, constituting a fundamental component for assessing regional landslide susceptibility. Subsequently, landslide susceptibility mapping was conducted based on pre-identified criteria considered relevant in associated environmental contexts. Eleven causal factors were determined, including elevation, slope, aspect, curvature, relative relief, lithology, precipitation, distance to drainage, distance to road, NDVI, land use, and vegetation cover. To generate the ultimate landslide susceptibility maps employing the FR and AHP methodologies (Fig.2), all thematic data layers were converted into a 30×30 m raster spatial database within the ArcGIS environment, utilizing the UTM zone 30 N coordinate system.

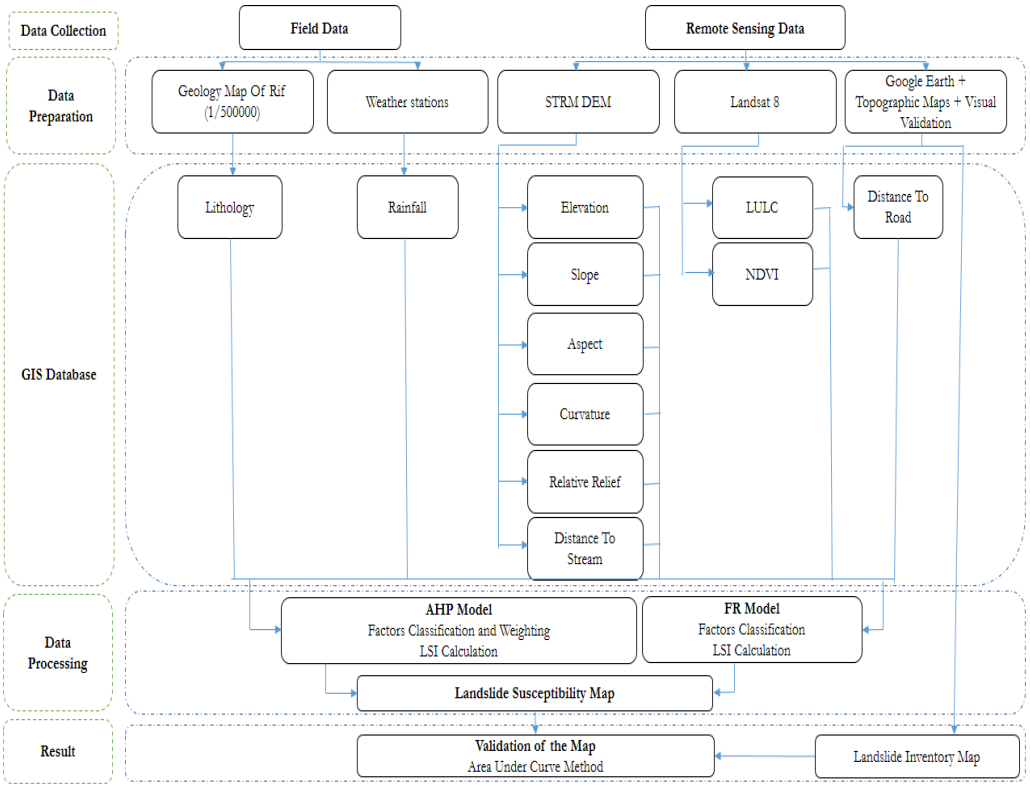

Figure 2: Schematic illustration of methods

2.3 Factors causal to landslides

Landslide susceptibility is primarily associated with the eleven factors presented in Table 1. These factors considered in this analysis were classified into three categories: data derived from the DEM, lithological characteristics extracted from the geological map after digitization, and drainage network features. A spatial database was developed in the ArcGIS environment, comprising eleven thematic layers, each representing a determinant factor in the landslide process (Fig.2).

2.4 Analytical Hierarchy Process (AHP) method

The AHP method, developed by Saaty (1977), represents a multicriteria analysis approach that allows for the quantification of qualitative characteristics through weighting [38], [39], [40]. This method has been successful in various fields, such as studying potential land use transformation [41] or evaluating the probability of water erosion [42].

The AHP consists of several phases, including structuring the problem hierarchically by defining the objective and prioritizing criteria and sub-criteria through a pairwise comparative analysis of each characteristic [43], [44], [45]. A standard scale from one to nine was employed to establish relative ranking values for all factors. On this scale, 1 represents equal importance, 3 indicates low importance, 5 reflects moderate importance, 7 denotes high importance, and 9 represents extreme importance. Intermediate values 2, 4, 6, and 8 were assigned to factors based on their relevance compared to others [46].

Once the comparison matrix is filled, the eigenvalues and corresponding eigenvectors are computed. The eigenvector reveals the priority order or hierarchy of the examined characteristics [38]. This result is paramount in evaluating probability, as it will determine the relative importance of each criterion at play. The eigenvalue serves as a measure to calculate the consistency ratio (CR) and the consistency index (CI) Eq. (1) [46].

$$CR = \frac{CI}{RI} \quad (1)$$

CR denotes the Consistency Ratio, RI stands for the random index, and CI represents the consistency index, formulated as Eq. (2) [46].

$$CI = (\lambda max - n)/(n - 1) \quad (2)$$

λmax represents the largest or principal eigenvalue of the matrix, easily computable from the matrix, while n denotes the order of the matrix.

Using equation (3) [46], the weights obtained were allocated to the various causal classes to create a distinctive landslide susceptibility index.

$$LSI = \sum Ri * Wi \quad (3)$$

Ri represents the landslide-influencing factor, and Wi denotes the criteria weights for each factor.

2.5 Frequency ratio (FR) method

The Frequency Ratio (FR) is a recognized bivariate statistical method known for its simplicity of implementation and accurate results. It is commonly employed in mapping landslide susceptibility [47], [48]. FR is based on the assumption that future landslide events will occur under similar conditions to past events. A landslide inventory and thematic maps combination was developed using Eq. (4)[48] to obtain an FR for each class of causal factors.

$$FR = \frac{N\ pix(1)/N\ pix\ (2)}{\sum N\ pix\ (3)\ /\ \sum N\ Pix\ (4)} \quad (4)$$

Npix 1 represents the area of landslide in each class, N pix 2 denotes the area of the class, N pix 3 signifies the total number of area landslide pixels over the entire area, and N pix 4 indicates the total number of pixels in the area.

The Landslide Susceptibility Index (LSI) was then calculated by summing the values of each factor ratio using Eq. (5).

$$LSI = FR1 + FR2 + FR3 + \cdots + FRn \quad (5)$$

Where FR is the frequency ratio for each factor.

According to the FR method, one equals the average value. Thus, an FR less than 1 indicates an average correlation, while an FR greater than 1 indicates a higher correlation, suggesting an increased risk of landslide [49], [50], [51].

3. Results and Discussions

Using a GIS environment, the AHP maps landslide susceptibility in the Oued Lebene watershed. An inventory of 70 landslides was established from Google Earth data and field observations (Fig.3). The impact of different factors on landslide distribution was conducted by comparing these causal factors based on the existing landslide inventory. The results obtained from the AHP comparison matrix (Table 2) show, on the one hand, that the consistency ratio was less than 10%. On the other hand, the maximum weighting was recorded by the elevation, slope, and lithology factors at 0.217, 0.157, and 0.134, respectively. Factors represented by curvature, precipitation, and terrain aspects have significantly impacted the spatial distribution of landslide susceptibility. Meanwhile, proximity to roads, proximity to drainage networks, land use, and NDVI have little influence on landslide occurrence.

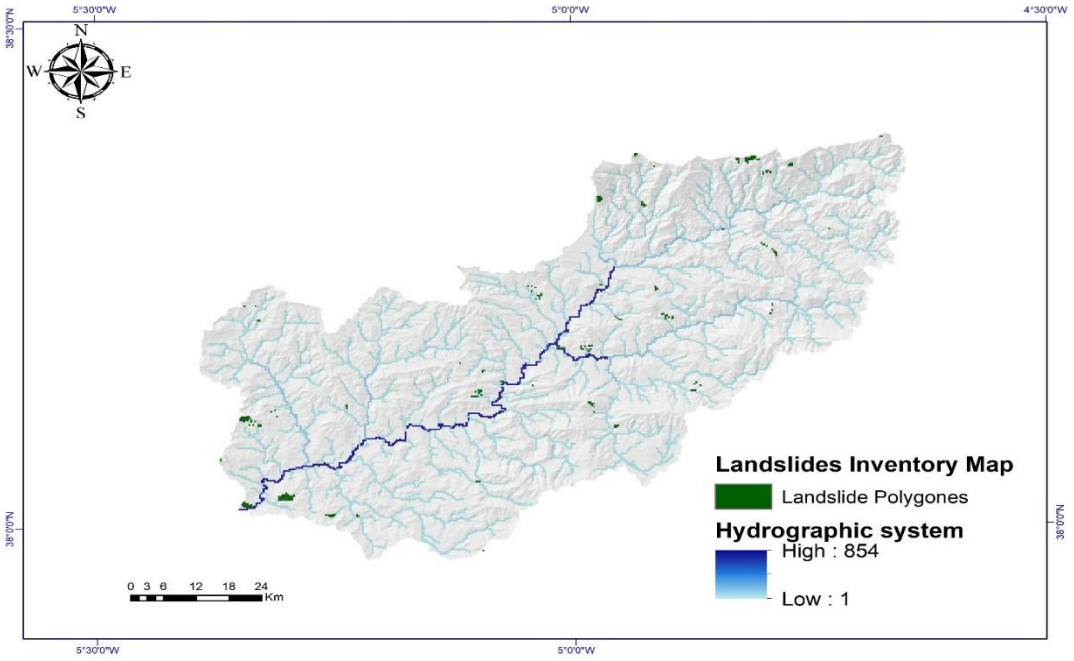

Figure 3: Landslides inventory map

Table 2: Thematic factors comparison through the pair-wise matrix

Factors	Elevation	Slope	Lithology	Curvature	Rainfall	Aspect	Distance To Stream	Distance To Road	LULC	NDVI	Relative Relief	Wi
Elevation	1	2	3	2	2	3	5	7	5	5	9	0.217
Slope	1/2	1	2	2	2	3	3	4	4	5	7	0.157
Lithology	1/3	1/2	1	3	3	2	2	2	4	5	6	0.134
Curvature	1/2	1/2	1/3	1	2	3	4	5	4	5	6	0.127
Rainfall	1/2	1/2	1/3	1/2	1	3	3	4	4	4	6	0.107
Aspect	1/3	1/3	1/2	1/3	1/3	1	2	3	4	5	6	0.079
Distance To Stream	1/5	1/3	1/2	1/4	1/3	1/2	1	2	2	4	4	0.054
Distance To Road	1/7	1/4	1/2	1/5	1/4	1/3	1/2	1	3	4	4	0.045
LULC	1/5	1/4	1/4	1/4	1/4	1/4	1/2	1/3	1	3	4	0.036
NDVI	1/5	1/5	1/5	1/5	1/4	1/5	1/4	1/4	1/3	1	6	0.029
Relative Relief	1/9	1/7	1/6	1/6	1/6	1/6	1/4	1/4	1/4	1/6	1	0.015
□max = 12.4522 CI = 0.1452 CR= 0.0955												

Table 3: Factors weights and consistency ratio obtained from AHP

Factors	Class	Final Weight	λmax	CI	CR
Elevation	140 -340	0.131	5.0944	0.0236	0.021
	350 - 510	0.355			
	520 - 700	0.031			
	710 - 970	0.156			
	980 - 1707	0.327			
Slope	0 - 6.7	0.068	5.0935	0.0233	0.0208
	6.8 - 13	0.112			
	14 - 19	0.530			
	20 - 27	0.068			
	28 - 65	0.222			
Lithology	Litharenite and sandy marl	0.210	9.7128	0.0891	0.0614
	Sandy marl and limestone marl	0.237			
	Black pelite, limestone intercalation	0.213			
	White limestone marl with flint	0.115			
	Marly matrix	0.085			
	Terraces and alluvial	0.061			
	Alternation of oolitic limestone and dolomitic breccia	0.038			
	Chaotic facies with reworking and sedimentary clippers of prerif	0.024			
	Conglomerates, sandstones, and marls	0.017			
Aspect	Flat (-1)	0.202	10.8782	0.0975	0.0646
	North (0-22.5)	0.225			
	Northeast (22.5-67.5)	0.205			
	East (67.5-112.5)	0.118			
	Southeast (112.5-157.5)	0.084			
	South (157.5-202.5)	0.059			
	Southwest (202.5-247.5)	0.040			
	West (247.5-292.5)	0.022			
	Northwest (292.5-337.5)	0.016			
	North (337.5-360)	0.029			
Curvature	Concave	0.067	3	0	0
	Flat	0.467			
	Convex	0.467			
Rainfall	236 - 377	0.122	5.1214	0.0303	0.027
	378 - 465	0.258			
	466 - 550	0.079			
	551 - 622	0.079			
	623 - 807	0.462			
Relative Relief	0 -150	0.182	3.0879	0.0439	0.075
	160 - 190	0.115			
	200 - 250	0.703			

LULC	Water	0.035	6.4383	0.0876	0.0706
	Forest	0.054			
	Irrigated Agriculture	0.085			
	Built	0.085			
	Bare Grounds	0.145			
	Agriculture Lands	0.595			
NDVI	Dead plants or object	0.228	4.0797	0.0265	0.0295
	Unhealthy Vegetation	0.600			
	Moderate Healthy Vegetation	0.121			
	Very Healthy Vegetation	0.051			
Distance To Road	200	0.579	6.5193	0.1038	0.0837
	400	0 .145			
	600	0.093			
	800	0.093			
	1000	0.059			
	>1000	0.031			
Distance To Stream	100	0.489	6.5548	0.1109	0.0894
	400	0.151			
	700	0.151			
	1000	0.100			
	1500	0.070			
	>1500	0.041			

3.1 Factors Ranking using AHP

The elevation factor and an increasing slope gradient directly impact the degree of weathering and erosion rate. Areas with low altitudes and gentle slopes are less susceptible to landslides than high-altitude areas with steep slopes [52].

The spatial distribution relationship aligns perfectly between elevation and slope; Table 3 and Fig. 4a and 4b demonstrate that the maximum weighting of these two factors was recorded in the moderate elevation and slope class, respectively 0.355 and 0.530, and in the extreme class with 0.327 and 0.222. High-slope and elevation terrains are highly susceptible to landslides [53]. The moderate elevation and slope class are prone to this hazard in the watershed.

The Oued Lebene watershed was primarily composed of nine lithological formation categories, almost entirely characterized by the dominance of marls, which were contributed through their structures to the instability of the study area regarding landslides with a weight exceeding 0.5 (Table 3 and Fig. 6c).

The profile curvature describes the rate of change in the slope of a terrain [54]. A dense drainage network resulting in high concavity or convexity always leads to slope failure and landslide susceptibility [55]. The study area in question experiences an equal effect from the Flat class and the Convex class with a weight of 0.467, while the impact of the Concave class is minor (Table 3 and Fig.4d).

Intense precipitation implies maximum erosivity, significantly affecting slope instability concerning landslide occurrence. The values of this factor for the Oued Leben watershed range from 236 to 807 mm/year, showing an increasing trend from downstream to upstream. The maximum values are located upstream to the east and northwest; hence, the maximum weight of the [623 - 807] class was quantified at 0.462 (Table 3 and Fig.5b).

The initiation of a landslide was closely related to the aspect that reflects the direction of the slope [56]. The results shown in Table 2 and Fig. 4c indicate that this factor has a moderate impact on the landslide process with a weighting of 0.079. Among the different aspect factor classes, the classes corresponding to the North and East parts of the study area (North, East, and Northeast) were considered more significant than others, with weights of 0.225, 0.118, and 0.205, respectively (Table 3).

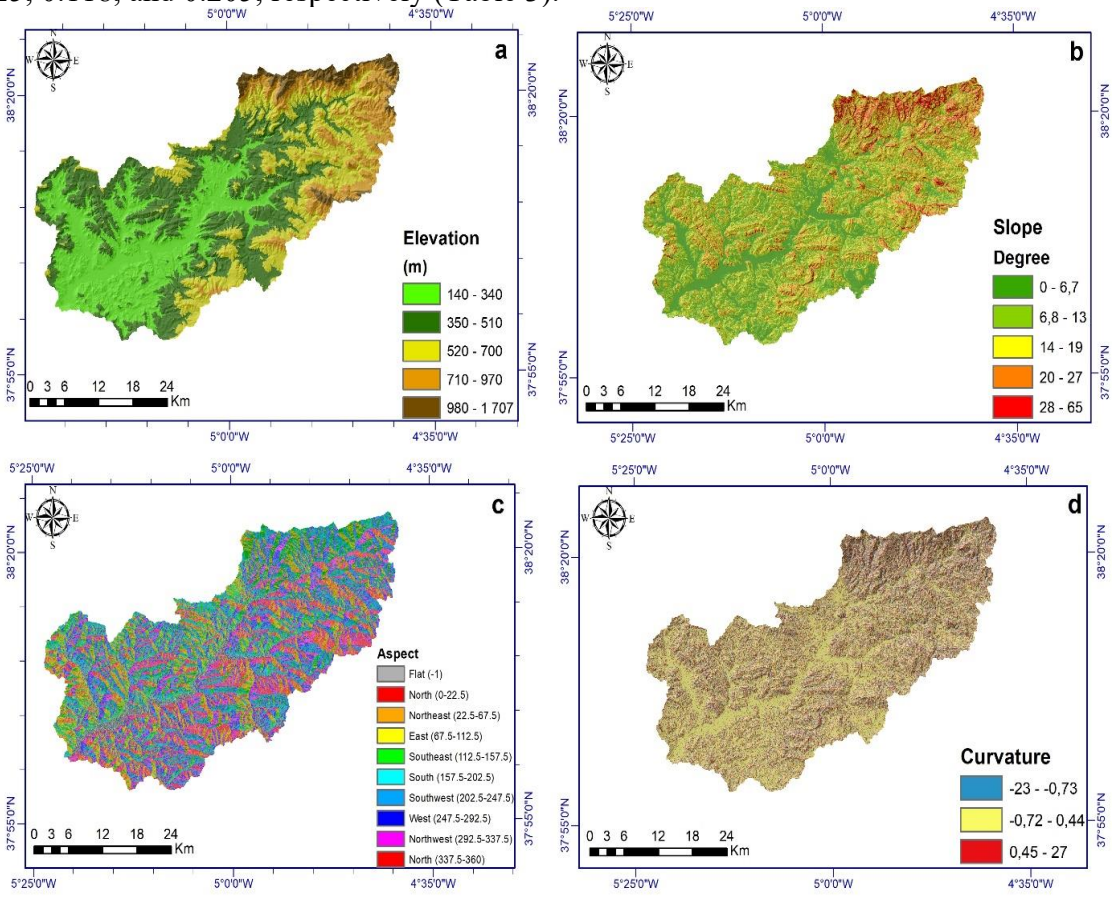

Figure 4: Map of oued Lebene watershed: (a) Elevation, (b) Slope, (c) Aspect, and (d) Curvature

Streams contribute to slope destabilization in rugged areas, causing undercutting of the slope base through their fluvial action [57]. The final weight of this factor is approximately 0.054, implying a minimal influence on the spatial distribution of landslides in watersheds (Table 2). The analysis of the results in Table 3 and Fig. 6b shows that the class referring to areas near watercourses within a range of less than 100 m had a significant impact compared to other classes, with the impact decreasing progressively as one moves away from the rivers.

As for the other factors responsible for the spatial distribution of landslides in the Oued Lebene watershed, it was observed that their final weights do not exceed 0.045 for the proximity to road networks, following the same logic as proximity to watercourses (Table 2 and Fig. 6a). Land use and NDVI have minimal influence on landslide susceptibility, with respective final weights of approximately 0.036 and 0.029 (Table 2, Fig. 5c and Fig. 5d). The

least significant factor in this process is relative relief, which implies the impact of vegetation changes relative to elevation, with a final weight of 0.015 (Table 2 and Fig. 5a).

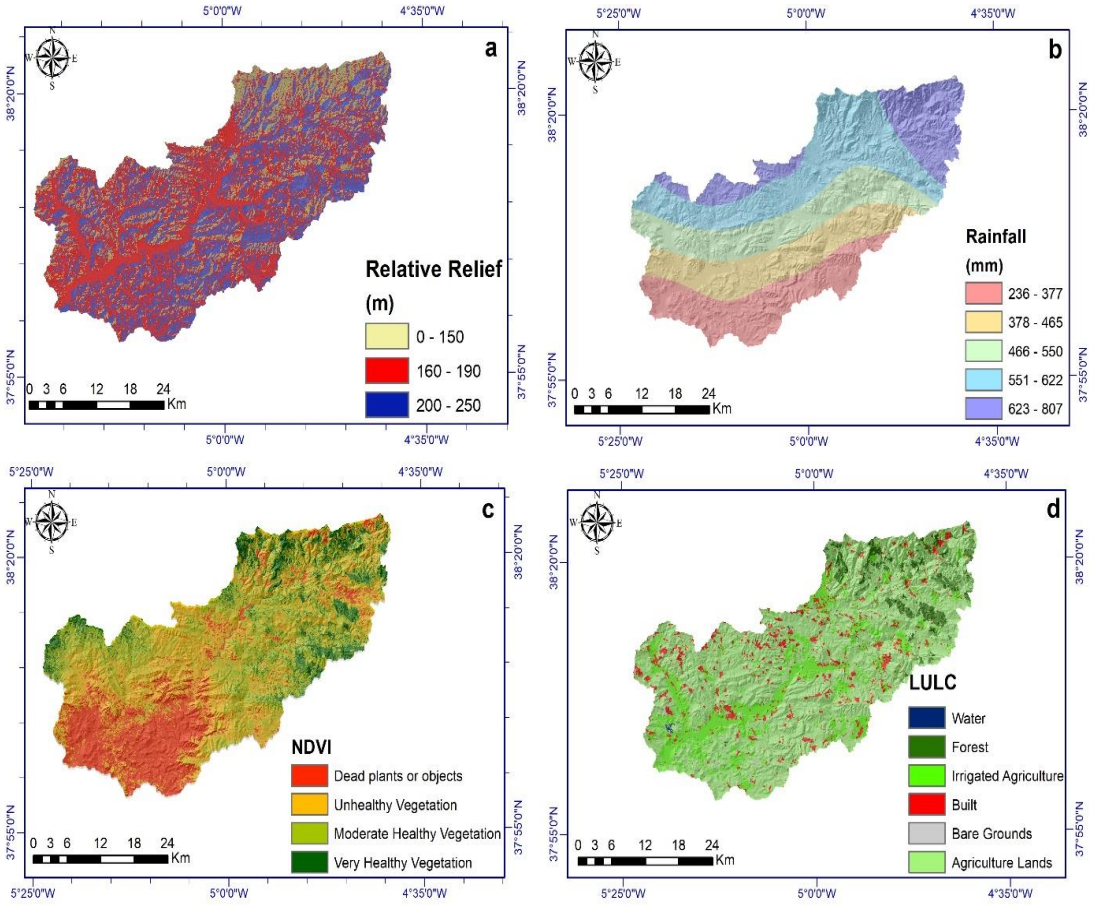

Figure 5: Map of oued Lebene watershed: (a) Relative Relief, (b) Rainfall, (c) NDVI, and (d) LULC

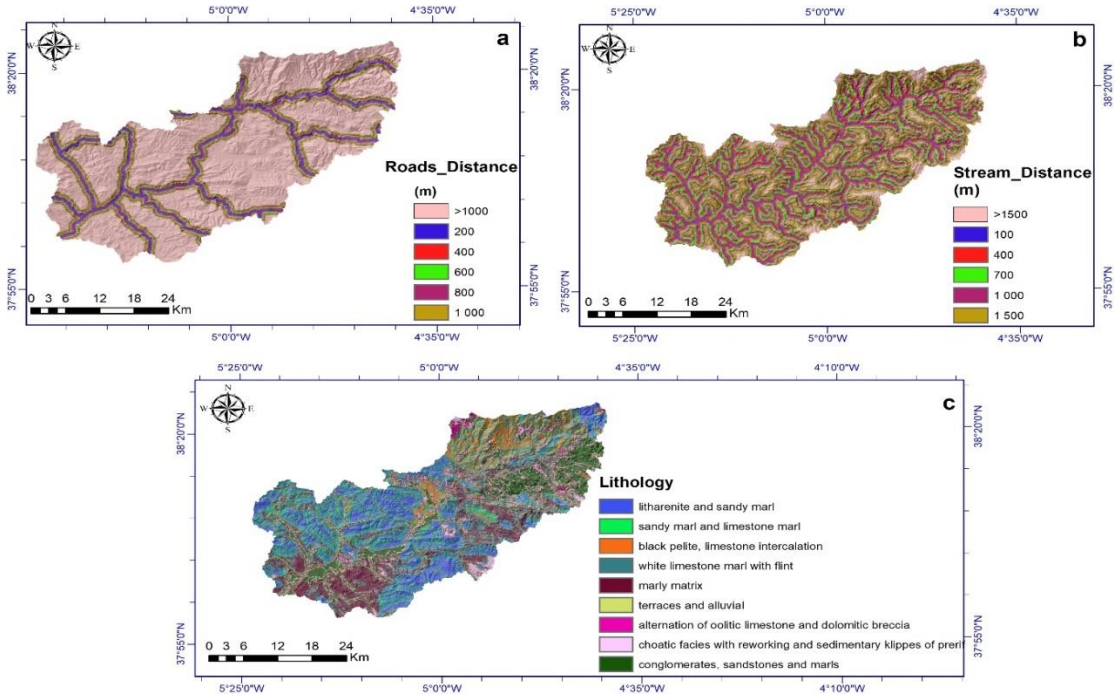

Figure 6: Map of Oued Lebene watershed: (a) Distance to Road, (b) Distance to Stream, and (c) Lithology

3.2 Factors Ranking using FR

The Frequency Ratio (FR) is a method derived from probabilistic approaches based on observed correlations between the distribution of landslides and associated causal factors [58], [59]. The Frequency Ratio (FR) calculated value represents the correlation level between landslides and a particular class of causal factor [60].

The analysis of Table 4 shows that the vegetation cover factor and the NDVI have considerably impacted landslides with the highest frequency ratio, 4.786 and 4.349, respectively. Dense vegetation cover contributes to mitigating soil movement while promoting soil horizon stability. Hence, the probability of landslide occurrence is high in areas where vegetation is absent, as illustrated by the bare soil class for the LULC factor and the Dead plants or objects class for the NDVI factor. In third and fourth place, find slope and elevation, which act in synchronization, where the frequency ratio gradually increases with the growth of the angle and altitude, with a final weight of approximately 3.689 and 3.156, respectively.

The distance from roads and drainage networks denotes a moderate susceptibility probability, followed by an aspect with a value of around 1.451, which remains moderate compared to other factors. Meanwhile, lithology, with a weight of 1.034, was characterized by complex geological structures. Hence, classes present significant values, including formations such as marls. As for precipitation and curvature, the results indicate a minor contribution and a lower possibility for landslides.

Table 4: Weight calculation for each class through FR

Factors	Class	Class Pixels	Landslide Pixels	FR	Poids
Slope (Degree)	0 - 6,7	382548	963	0,003	**3,689**
	6,8 - 13	517895	1908	0,004	
	14 - 19	452603	2154	0,005	
	20 - 27	266772	2034	0,008	
	28 - 65	88334	1158	0,013	
Total		1708152	8217	0,019	
Elevation(m)	140 - 340	508589	3269	0,006	**3,156**
	350 - 510	581702	2169	0,004	
	520 - 700	355493	815	0,002	
	710 - 970	192353	610	0,003	
	980 - 1707	70015	1354	0,019	
Total		1708152	8217	0,035	
Lithology	Litharenite and sandy marl	453345	2078	0,005	**1,034**
	Sandy marl and limestone marl	299320	1652	0,006	
	Black pelite, limestone intercalation	196177	1123	0,006	
	White limestone marl with flint	158450	641	0,004	
	marly matrix	235077	1521	0,006	
	Terraces and alluvial	56292	251	0,004	
	Alternation of oolitic limestone and dolomitic breccia	60000	507	0,008	
	Chaotic facies with reworking and sedimentary clippers of prerif	75561	123	0,002	
	Conglomerates, sandstones, and marls	174607	319	0,002	

Total		1708829	8215	0,043	
Aspect	Flat (-1)	1379	3	0,002	**1,451**
	North (0-22.5)	113856	168	0,001	
	Northeast (22.5-67.5)	191920	452	0,002	
	East (67.5-112.5)	183494	460	0,003	
	Southeast (112.5-157.5)	203622	1426	0,007	
	South (157.5-202.5)	250835	2527	0,010	
	Southwest (202.5-247.5)	234934	1998	0,009	
	West (247.5-292.5)	216309	800	0,004	
	Northwest (292.5-337.5)	204867	269	0,001	
	North (337.5-360)	106936	114	0,001	
Total		1708152	8217	0,040	
Curvature	Concave (-23 - -0,73)	281874	1873	0,007	**1,000**
	Plane (-0,72 - 0,44)	994669	4170	0,004	
	Convex (0,45 - 27)	431609	2174	0,005	
Total		1708152	8217	0,016	
Rainfall (mm)	236 - 377	290259	2045	0,007	**1,026**
	378 - 465	275883	1106	0,004	
	466 - 550	299574	1663	0,006	
	551 - 622	420844	1346	0,003	
	623 - 807	255000	1139	0,004	
Total		1541560	7299	0,024	
Relative Relief (m)	0 - 150	316219	3145	0,010	**3,002**
	160 - 190	802612	3813	0,005	
	200 - 250	579282	1239	0,002	
Total		1698113	8197	0,017	
LULC	Forest	73556	29	0,000	**4,786**
	Irrigated Agriculture	276797	1051	0,004	
	Built	106237	129	0,001	
	Bare Grounds	10131	327	0,032	
	Agriculture Lands	1073290	5838	0,005	
Total		1540011	7374	0,043	
NDVI	Dead plants or objects	347991	4380	0,013	**4,349**
	Unhealthy Vegetation	563622	2426	0,004	
	Moderate Healthy Vegetation	463917	501	0,001	
	Very Healthy Vegetation	166506	51	0,000	
Total		1542036	7358	0,018	
Distance To Roads (m)	200	1029843	5780	0,006	**1,607**
	400	114223	66	0,001	
	600	107498	156	0,001	
	800	101266	401	0,004	
	1000	97105	394	0,004	
	>1000	91904	546	0,006	
Total		1541839	7343	0,022	
Distance To Stream	100	99671	1034	0,010	

(m)	400	149306	401	0,003	
	700	402313	1358	0,003	
	1000	345772	1324	0,004	
	1500	275706	1609	0,006	
	>1500	269071	1617	0,006	**1,550**
Total		1541839	7343	0,032	

3.3 AHP and FR for landslide susceptibility mapping

Once the factors weighted by class were determined, based on the final weight calculated for each class by each method, these factors were combined using the weighted sum tool in ArcGIS to produce landslide susceptibility maps of the study area. These maps were categorized into four classes describing susceptibility ranging from low to very high for landslide occurrence in the study area (Fig.7).

The analysis of the landslide susceptibility map produced by the AHP shows that 7.84% of the study area exhibits remarkable stability and faces a low risk of landslide occurrence. 70.56 % of the watershed falls into the moderate risk class. Meanwhile, 21.24% of the total area of this region faces a high risk, with only 0.36 % located in a very high-risk zone.

The landslide susceptibility map from the FR method shows a spatial distribution of risk classified as low to moderate, comprising 56.03% and 38.39% of the study area, respectively. Approximately 2.5% are susceptible, with nearly 0.1% facing a very high risk of landslide occurrence.

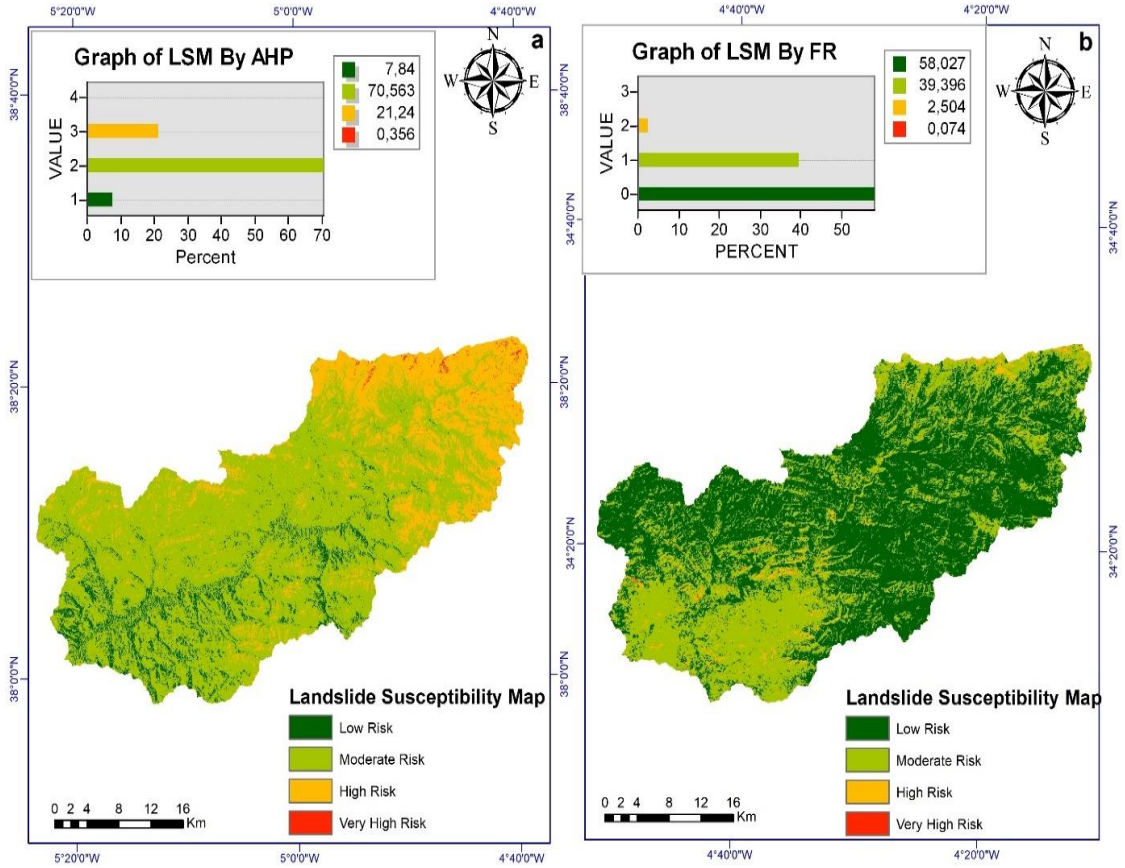

Figure 7: Landslide susceptibility Map of Oued Lebene watershed: (a) AHP Model, (b) FR Model

3.4 Assessment of the accuracy of the landslide susceptibility map

The landslides identified in the study area were randomly divided into two groups. Among the 70 landslides, 44 (70%) were chosen randomly as Training data, leaving the remaining 26 (30%) for validation (Testing data). AUC values range from 0 to 1, where values exceeding 0.5 suggest high predictive accuracy, while those below 0.5 suggest low predictive accuracy [61]. The calculation of the prediction rate revealed AUC values of approximately 0.722 using the FR method, slightly surpassing the AUC values of 0.711 obtained with the AHP method. The AUC findings from this study demonstrate satisfactory performance for both methods employed in landslide susceptibility mapping, albeit with the FR method showing a slight superiority over AHP. This is primarily due to the lack of literature and studies on this topic in the study area, and thus, the pairwise comparison was based on the inventory of existing landslides rather than expert judgments.

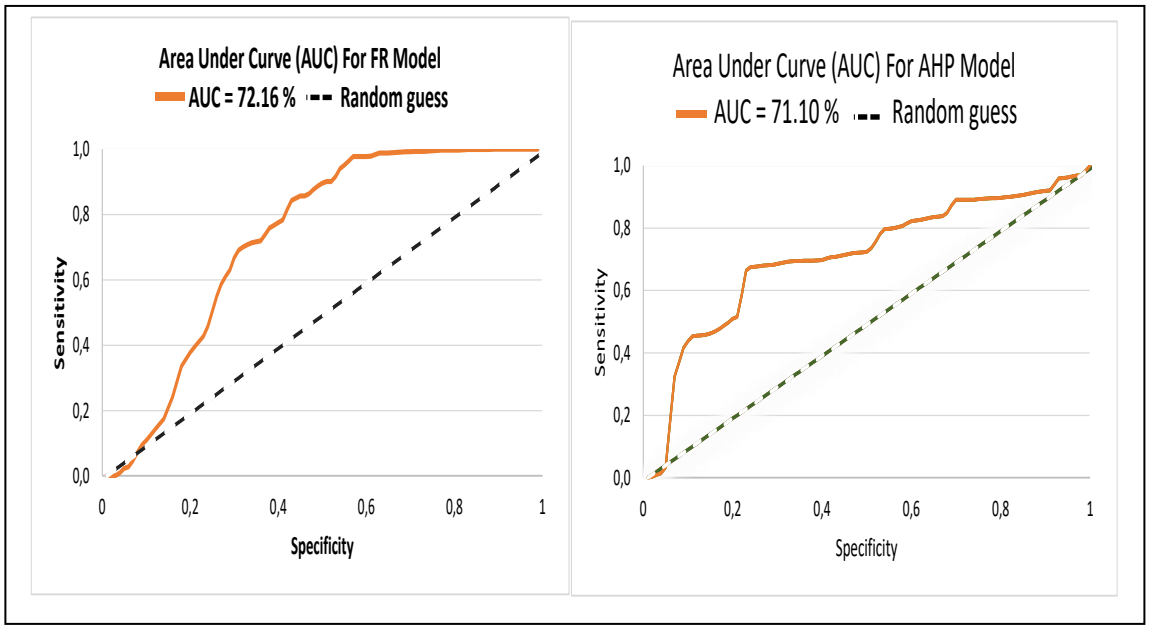

Figure 8: AUC for AHP and FR Model

4. Conclusion

According to the AHP approach, regions categorized as high, high, moderate, and low susceptibility represent 0.36%, 21.24%, 70.57%, and 7.84% of the total area, respectively. Similarly, the FR method indicates that areas classified as very high, high, moderate, and low susceptibility account for 0.08%, 2.50%, 39.39%, and 58.03% of the study area, respectively.

Following this, the modeling techniques for this hazard were assessed using the Area Under the Curve (AUC), revealing prediction rates of around 0.711 and 0.722 for AHP and FR, respectively. The outcomes of this validation demonstrated that the FR method slightly outperformed the AHP method.

The produced landslide maps could be valuable for relevant authorities, natural resource managers, and planners in planning development schemes and implementing landslide risk mitigation measures. Thus, increased attention should be paid to infrastructure in high-risk areas to reduce landslide losses. In conclusion, the future use of remote sensing data could constitute a significant contribution with geospatial techniques to establish landslide deformation zones in the study region.

References

[1] D. Brunsden et J. B. Thornes, "Landscape Sensitivity and Change," *Trans. Inst. Br. Geogr.*, vol. 4, nº 4, p. 463-484, 1979, doi: 10.2307/622210.

[2] H. Shen, H. Klapperich, S. M. Abbas, et A. Ibrahim., "Slope stability analysis based on the integration of GIS and numerical simulation," *Autom. Constr.*, vol. 26, p. 46-53, oct. 2012, doi: 10.1016/j.autcon.2012.04.016.

[3] J. Zhuang, J. Peng, G. Wang, I. Javed, Y. Wang, et W. Li, "Distribution and characteristics of landslide in Loess Plateau: A case study in Shaanxi province, " *Eng. Geol.*, vol. 236, p. 89-96, mars 2018, doi: 10.1016/j.enggeo.2017.03.001.

[4] S. Ali, P. Biermanns, R. Haider, et K. Reicherter, " Landslide susceptibility mapping by using a geographic information system (GIS) along the China–Pakistan Economic Corridor (Karakoram Highway), Pakistan," *Nat. Hazards Earth Syst. Sci.*, vol. 19, nº 5, p. 999-1022, mai 2019, doi: 10.5194/nhess-19-999-2019.

[5] A. Cubito, V. Ferrara, et G. Pappalardo, "Landslide hazard in the Nebrodi Mountains (Northeastern Sicily)," *Geomorphology*, vol. 66, nº 1, p. 359-372, mars 2005, doi: 10.1016/j.geomorph.2004.09.020.

[6] Y. Gao et E. C. Alexander, "Sinkhole hazard assessment in Minnesota using a decision tree model," *Environ. Geol.*, vol. 54, nº 5, p. 945-956, mai 2008, doi: 10.1007/s00254-007-0897-1.

[7] M. Moradi, M. H. Bazyar, et Z. Mohammadi, "GIS-based landslide susceptibility mapping by AHP method, a case study, Dena City, Iran," *J Basic Appl Sci Res*, vol. 2, p. 6715-6723, janv. 2012.

[8] D. W. Park, N. V. Nikhil, et S. R. Lee, "Landslide and debris flow susceptibility zonation using TRIGRS for the 2011 Seoul landslide event," *Nat. Hazards Earth Syst. Sci.*, vol. 13, nº 11, p. 2833-2849, nov. 2013, doi: 10.5194/nhess-13-2833-2013.

[9] H. Zhang *et al.*, "Extension of a GIS procedure for calculating the RUSLE equation LS factor," *Comput. Geosci.*, vol. 52, p. 177-188, mars 2013, doi: 10.1016/j.cageo.2012.09.027.

[10] L. Azeez, "Qurain AL-Thamad Valley Hydrological Aspects Extraction Using Remote Sensing and GIS Techniques," *Iraqi J. Sci.*, p. 2280-2287, Oct. 2019, doi: 10.24996/ijs.2019.60.10.22.

[11] M. J. García-Rodríguez, J. A. Malpica, B. Benito, et M. Díaz, "Susceptibility assessment of earthquake-triggered landslides in El Salvador using logistic regression," *Geomorphology*, vol. 95, nº 3, p. 172-191, mars 2008, doi: 10.1016/j.geomorph.2007.06.001.

[12] M. Xie, T. Esaki, G. Zhou, et Y. Mitani, "Geographic Information Systems-Based Three-Dimensional Critical Slope Stability Analysis and Landslide Hazard Assessment," J. Geotech. Geoenvironmental Eng., vol. 129, no 12, p. 1109-1118, déc. 2003, doi: 10.1061/(ASCE)1090-0241(2003)129:12(1109).

[13] D. J. Varnes, "The principles and practice of landslide hazard zonation," Bull. Int. Assoc. Eng. Geol. - Bull. Assoc. Int. Géologie Ing., vol. 23, no 1, p. 13-14, juin 1981, doi: 10.1007/BF02594720.

[14] S. Lee et B. Pradhan, "Probabilistic landslide hazards and risk mapping on Penang Island, Malaysia," *J. Earth Syst. Sci.*, vol. 115, nº 6, p. 661-672, déc. 2006, doi: 10.1007/s12040-006-0004-0.

[15] S. Z. Mousavi, A. Kavian, K. Soleimani, S. R. Mousavi, et al., "GIS-based spatial prediction of landslide susceptibility using logistic regression model," *Geomat. Nat. Hazards Risk*, vol. 2, nº 1, p. 33-50, mars 2011, doi: 10.1080/19475705.2010.532975.

[16] T. T. Al-Samarrai, "Engineering Geological Assessment for Rock Slope Stability of Chosen Areas from SW of Haibat Sultan Mountain, Kalkasmak-Koisanjaq Road / Iraq," *Iraqi J. Sci.*, p. 956-963, 2016.

[17] G.Champetier, "La cartographie des mouvements de terrain. Des cartes ZERMOS aux PER. Bulletin de liaison des labo des ponts et chaussées," *1987*, 1987.

[18] F. Guzzetti, P. Reichenbach, M. Cardinali, M. Galli, et F. Ardizzone, "Probabilistic landslide hazard assessment at the basin scale," *Geomorphology*, vol. 72, nº 1, p. 272-299, déc. 2005, doi: 10.1016/j.geomorph.2005.06.002.

[19] B. Pradhan, "Remote sensing and GIS-based landslide hazard analysis and cross-validation using multivariate logistic regression model on three test areas in Malaysia," *Adv. Space Res.*, vol. 45, nº 10, p. 1244-1256, mai 2010, doi: 10.1016/j.asr.2010.01.006.

[20] B. Pradhan et S. Lee, "Landslide susceptibility assessment and factor effect analysis: backpropagation artificial neural networks and their comparison with frequency ratio and bivariate logistic regression modeling," *Environ. Model. Softw.*, vol. 25, nº 6, p. 747-759, Jun 2010, doi: 10.1016/j.envsoft.2009.10.016.

[21] B. Khallef, "Mapping of Soil Erosion Using Remote Sensing and GIS: Case of The Oued Bouhamdane Watershed (North-East of Algeria)," *Iraqi J. Sci.*, p. 3691-3704, juill. 2023, doi: 10.24996/ijs.2023.64.7.44.

[22] D. Asmare, "Landslide hazard zonation and evaluation around Debre Markos town, NW Ethiopia—a GIS-based bivariate statistical approach," *Sci. Afr.*, vol. 15, p. e01129, mars 2022, doi: 10.1016/j.sciaf.2022.e01129.

[23] J. Remondo, J. Bonachea, et A. Cendrero, "A statistical approach to landslide risk modeling at basin scale: from landslide susceptibility to quantitative risk assessment," *Landslides*, vol. 2, nº 4, p. 321-328, déc. 2005, doi: 10.1007/s10346-005-0016-x.

[24] W. C. HANEBERG, "A Rational Probabilistic Method for Spatially Distributed Landslide Hazard Assessment," *Environ. Eng. Geosci.*, vol. 10, nº 1, p. 27-43, janv. 2004, doi: 10.2113/10.1.27.

[25] S. Lari, P. Frattini, et G. B. Crosta, "A probabilistic approach for landslide hazard analysis," *Eng. Geol.*, vol. 182, p. 3-14, nov. 2014, doi: 10.1016/j.enggeo.2014.07.015.

[26] F. Cervi, M. Berti, L. Borgatti, F. Ronchetti, F. Manenti, et A. Corsini, "Comparing predictive capability of statistical and deterministic methods for landslide susceptibility mapping: a case study in the northern Apennines (Reggio Emilia Province, Italy)," *Landslides*, vol. 7, nº 4, p. 433-444, déc. 2010, doi: 10.1007/s10346-010-0207-y.

[27] D. Asmare, "Application and validation of AHP and FR methods for landslide susceptibility mapping around choke mountain, northwestern Ethiopia," *Sci. Afr.*, vol. 19, p. e01470, mars 2023, doi: 10.1016/j.sciaf.2022.e01470.

[28] J. Efiong, D. I. Eni, J. N. Obiefuna, et S. J. Etu, "Geospatial modeling of landslide susceptibility in Cross River State of Nigeria," *Sci. Afr.*, vol. 14, p. e01032, nov. 2021, doi: 10.1016/j.sciaf.2021.e01032.

[29] L. C. Tuan, T. T. T. Trang, P. T. Hieu, et T. N. H. Vi, "Landslides Study in Bac Can Province, Vietnam by Analytic Hierarchy Process Method," *Iraqi J. Sci.*, p. 5691-5706, nov. 2023, doi: 10.24996/ijs.2023.64.11.19.

[30] S. Moragues, M. G. Lenzano, M. Lanfri, S. Moreiras, E. Lannutti, et L. Lenzano, "Analytic hierarchy process applied to landslide susceptibility mapping of the North Branch of Argentino Lake, Argentina," *Nat. Hazards*, vol. 105, nº 1, p. 915-941, janv. 2021, doi: 10.1007/s11069-020-04343-8.

[31] L. Strokova, "Landslide susceptibility zoning in surface coal mining areas: a case study Elga field in Russia," *Arab. J. Geosci.*, vol. 15, nº 2, p. 146, janv. 2022, doi: 10.1007/s12517-021-09314-2.

[32] M. S. Ahmad, MonaLisa, et S. Khan, "Comparative analysis of analytical hierarchy process (AHP) and frequency ratio (FR) models for landslide susceptibility mapping in Reshun, NW Pakistan, " *Kuwait J. Sci.*, vol. 50, nº 3, p. 387-398, juill. 2023, doi: 10.1016/j.kjs.2023.01.004.

[33] B. G. Babitha, "A framework employing the AHP and FR methods to assess the landslide susceptibility of the Western Ghats region in Kollam district," *Saf. Extreme Environ.*, vol. 4, nº 2, p. 171-191, août 2022, doi: 10.1007/s42797-022-00061-5.

[34] C. Tesfa, "GIS-Based AHP and FR Methods for Landslide Susceptibility Mapping in the Abay Gorge, Dejen–Renaissance Bridge, Central, Ethiopia," *Geotech. Geol. Eng.*, vol. 40, nº 10, p. 5029-5043, oct. 2022, doi: 10.1007/s10706-022-02197-4.

[35] N. Gupta, S. K. Pal, et J. Das, "GIS-based evolution and comparisons of landslide susceptibility mapping of the East Sikkim Himalaya," *Ann. GIS*, vol. 28, nº 3, p. 359-384, juill. 2022, doi: 10.1080/19475683.2022.2040587.

[36] A. Gartet et J. Gartet, "DÉGRADATION SPÉCIFIQUE ET TRANSPORTS SOLIDES DANS LE BASSIN DE L'OUED LEBÈNE (Prérif central, Maroc septentrional)," *Papeles Geogr.*, 2005.

[37] F. El Amarty, A. Lahrach, L. Benaabidate, et A. Chakir, "Estimating Soil Erosion and Sediment Yield Using Geographic Information System in the Central Pre-Rif (Northern Morocco) – The Case of the Oued Lebene Watershed," *Ecol. Eng. Environ. Technol.*, vol. 25, nº 8, p. 1-16, août 2024, doi: 10.12912/27197050/187977.

[38] T. L. Saaty, "Decision making with the analytic hierarchy process," *Int. J. Serv. Sci.*, vol. 1, nº 1, p. 83-98, janv. 2008, doi: 10.1504/IJSSCI.2008.017590.

[39] K. Ransikarbum et S. J. Mason, "Goal programming-based post-disaster decision making for integrated relief distribution and early-stage network restoration," *Int. J. Prod. Econ.*, vol. 182, p. 324-341, déc. 2016, doi: 10.1016/j.ijpe.2016.08.030.

[40] S. Panchal et K. Shrivastava, "Landslide hazard assessment using analytic hierarchy process (AHP): A case study of National Highway 5 in India," *Ain Shams Eng. J.*, vol. 13, nº 3, p. 101626, mai 2022, doi: 10.1016/j.asej.2021.10.021.

[41] M. M. Yagoub, T. AlSumaiti, Y. T. Tesfaldet, K. AlArfati, M. Alraeesi, et M. E. Alketbi, "Integration of Analytic Hierarchy Process (AHP) and Remote Sensing to Assess Threats to Preservation of the Oases: Case of Al Ain, UAE," *Land*, vol. 12, nº 7, Art. nº 7, juill. 2023, doi: 10.3390/land12071269.

[42] A. Halefom et A. Teshome, "Modelling and mapping of erosion potentiality watersheds using AHP and GIS technique: a case study of Alamata Watershed, South Tigray, Ethiopia," *Model. Earth Syst. Environ.*, vol. 5, nº 3, p. 819-831, sept. 2019, doi: 10.1007/s40808-018-00568-6.

[43] D. Myronidis, C. Papageorgiou, et S. Theophanous, "Landslide susceptibility mapping based on landslide history and analytic hierarchy process (AHP)," *Nat. Hazards*, vol. 81, nº 1, p. 245-263, mars 2016, doi: 10.1007/s11069-015-2075-1.

[44] A. Yalcin, "GIS-based landslide susceptibility mapping using analytical hierarchy process and bivariate statistics in Ardesen (Turkey): Comparisons of results and confirmations," *CATENA*, vol. 72, nº 1, p. 1-12, janv. 2008, doi: 10.1016/j.catena.2007.01.003.

[45] F. El Bchari, B. Theilen-Willige, et H. Ait Malek, "Landslide hazard zonation assessment using GIS analysis at the coastal area of Safi (Morocco)," *Proc. ICA*, vol. 2, p. 1-7, juill. 2019, doi: 10.5194/ica-proc-2-24-2019.

[46] T. L. Saaty, "How to make a decision: The analytic hierarchy process," *Eur. J. Oper. Res.*, vol. 48, nº 1, p. 9-26, sept. 1990, doi: 10.1016/0377-2217(90)90057-I.

[47] K. Xu, "Comparative study on landslide susceptibility mapping based on different ratios of training samples and testing samples by using RF and FR-RF models," *Nat. Hazards Res.*, juill. 2023, doi: 10.1016/j.nhres.2023.07.004.

[48] D. Ehret, "Frequency ratio analysis of mass movements in the Xiangxi catchment, Three Gorges Reservoir area, China," *J. Earth Sci.*, vol. 21, nº 6, p. 824-834, déc. 2010, doi: 10.1007/s12583-010-0134-9.

[49] L. Li, H. Lan, C. Guo, Y. Zhang, Q. Li, et Y. Wu, "A modified frequency ratio method for landslide susceptibility assessment," *Landslides*, vol. 14, nº 2, p. 727-741, avr. 2017, doi: 10.1007/s10346-016-0771-x.

[50] B. Li, N. Wang, et J. Chen, "GIS-Based Landslide Susceptibility Mapping Using Information, Frequency Ratio, and Artificial Neural Network Methods in Qinghai Province, Northwestern China," *Adv. Civ. Eng.*, vol. 2021, p. e4758062, juill. 2021, doi: 10.1155/2021/4758062.

[51] R. Anbalagan, R. Kumar, K. Lakshmanan, S. Parida, et S. Neethu, "Landslide hazard zonation mapping using frequency ratio and fuzzy logic approach, a case study of Lachung Valley, Sikkim," *Geoenvironmental Disasters*, vol. 2, nº 1, p. 6, févr. 2015, doi: 10.1186/s40677-014-0009-y.

[52] A. Kailas et G. Shajan, "Landslide Hazard Zonation (LHZ) Mapping of Attappady, Kerala using GIS," vol. 05, nº 03.

[53] J. Dou, « Evaluating GIS-Based Multiple Statistical Models and Data Mining for Earthquake and Rainfall-Induced Landslide Susceptibility Using the LiDAR DEM,» *Remote Sens.*, vol. 11, nº 6, Art. nº 6, janv. 2019, doi: 10.3390/rs11060638.

[54] C. Yilmaz, T. Topal, et M. L. Süzen, "GIS-based landslide susceptibility mapping using bivariate statistical analysis in Devrek (Zonguldak-Turkey)," *Environ. Earth Sci.*, vol. 65, nº 7, p. 2161-2178, avr. 2012, doi: 10.1007/s12665-011-1196-4.

[55] S. Mandal et K. Mandal., "Bivariate statistical index for landslide susceptibility mapping in the Rorachu river basin of eastern Sikkim Himalaya, India," *Spat. Inf. Res.*, vol. 26, nº 1, p. 59-75, févr. 2018, doi: 10.1007/s41324-017-0156-9.

[56] M. Basharat, J. Rohn, M. S. Baig, et M. R. Khan, "Spatial distribution analysis of mass movements triggered by the 2005 Kashmir earthquake in the Northeast Himalayas of Pakistan," *Geomorphology*, vol. 206, p. 203-214, févr. 2014, doi: 10.1016/j.geomorph.2013.09.025.

[57] C. van Westen, T. Gorum, X. Fan, R. Qiu Huang, Q. Xu, et C. Tang, "Distribution Pattern of Earthquake-induced Landslides Triggered by the 12 May 2008 Wenchuan Earthquake," p. 4437, Mai 2010.

[58] F. E. S. Silalahi, Pamela, Y. Arifianti, et F. Hidayat, "Landslide susceptibility assessment using frequency ratio model in Bogor, West Java, Indonesia," *Geosci. Lett.*, vol. 6, nº 1, p. 10, nov. 2019, doi: 10.1186/s40562-019-0140-4.

[59] A. Yalcin, S. Reis, A. C. Aydinoglu, et T. Yomralioglu, "A GIS-based comparative study of frequency ratio, analytical hierarchy process, bivariate statistics and logistics regression methods for landslide susceptibility mapping in Trabzon, NE Turkey," *CATENA*, vol. 85, nº 3, p. 274-287, juin 2011, doi: 10.1016/j.catena.2011.01.014.

[60] T. Mersha et M. Meten, "GIS-based landslide susceptibility mapping and assessment using bivariate statistical methods in Simada area, northwestern Ethiopia," *Geoenvironmental Disasters*, vol. 7, nº 1, p. 20, juin 2020, doi: 10.1186/s40677-020-00155-x.

[61] O. H. Ozioko et O. Igwe, "GIS-based landslide susceptibility mapping using heuristic and bivariate statistical methods for Iva Valley and environs Southeast Nigeria," *Environ. Monit. Assess.*, vol. 192, nº 2, p. 119, janv. 2020, doi: 10.1007/s10661-019-7951-9.